Journal of Thermal Analysis and Calorimetry
https://doi.org/10.1007/s10973-017-6892-1

Master decomposition curve of carbonaceous materials used in casting powders

E. Benavidez[1] · L. Santini[1] · A. Martín[1] · E. Brandaleze[1]

Received: 11 August 2017 / Accepted: 3 December 2017

Abstract
Casting powders are used in the continuous casting process of steels. These powders contain several oxides, fluoride compounds and carbonaceous materials. The decomposition kinetics of these carbonaceous materials regulates the melting rate of casting powders. In a previous work, a decomposition kinetics of two carbonaceous materials (coke and graphite) added to a casting powder was studied. Based on those data, in the present work, master decomposition curves (MDC) of these powders were constructed. For this, the values of both the activation energy (E) and the degree of decomposition (α), obtained in the thermogravimetric tests, were used for each heating rate (β). Then, the work of decomposition (θ_D) was calculated and the MDC was obtained. From the MDC, it was possible to predict the time (t) needed to produce a given degree of decomposition (α) at different temperatures (T). Taking this into account, it was possible to validate the master decomposition curves through different thermal treatments, where the degree of decomposition was calculated by interpolating the MDCs. These values were compared with those determined experimentally by measuring the mass loss in each heat treatment. In all cases, the results showed a good correlation between the predicted and measured values. It is concluded that the use of the MDC represents a useful tool to evaluate and compare the behavior of carbonaceous materials added to casting powder.

Keywords Master decomposition curve · Thermogravimetry · Carbonaceous materials · Casting powders

Introduction

Casting powders (also called mold powders or mold fluxes) are synthetic slags formed by a mix of several minerals such as wollastonite, feldspars, carbonates, quartz, and fluorite. The main oxides present in their compositions are silica (SiO_2), calcium oxide (CaO), sodium oxide (Na_2O), and the binary basicity (CaO/SiO_2 ratio) is between 0.7 and 1.3. They also contain fluorite (CaF_2) and free carbon (2–20 wt%) in their compositions [1]. Free carbon is incorporated through different carbonaceous materials such as graphite, petroleum coke and carbon black [2]. During the steel continuous casting process, these powders are added to the liquid steel surface (at $\approx$ 1650 °C) forming three different layers: powdered, sintered, and molten. The molten layer forms a "liquid slag pool". During casting process, this molten slag penetrates into the gap between the copper mold wall and the solidified steel shell. Thus, mold powders perform several functions depending on the specific contact zone: (a) in contact with the liquid steel (at the top of the mold) and (b) in contact with the solidified steel (in the area of the mold wall) [3]. In the zone of contact with the liquid steel, the functions of casting powders are: (1) thermal insulation, to avoid heat loss, (2) atmospheric protection, to avoid steel reoxidation, and (3) inclusions entrapment, to absorb inclusions in the interface slag–metal. In the zone of contact with solidified steel, these powders control (1) the lubrication, between the solidified steel shell and the mold, and (2) the heat transfer, from the steel to the mold [3].

The addition of carbonaceous material fulfills two important functions. In the first stage of the process, the carbonaceous material decomposes and forms CO_x (gas), which protects the steel surface from reoxidation. The

✉ E. Benavidez
ebenavidez@frsn.utn.edu.ar

[1] Department of Metallurgy & Centre DEYTEMA, Facultad Regional San Nicolás, Universidad Tecnológica Nacional, Colón 332 – (B2900LWH), San Nicolás, Argentina

Published online: 13 December 2017

second function is linked to the melting rate of the casting powder. Melting rate controls the depth of the liquid pool to ensure proper lubrication and uniform heat transfer during the solidification of the steel. For this reason, melting rate is one of the main properties to be considered in the design of casting powder [4].

Therefore, the main properties of these powders are: viscosity (for lubrication), kinetics of crystallization (for thermal extraction) and the melting rate (for the control of the liquid slag pool). This last property is the one considered in the present work. It depends on: the parameters of the industrial process, the chemical composition of mold powder, the percentage of carbon and those analyzed in the present work: the size, morphology and type of carbonaceous material added [5, 6].

In a previous work [7], the authors studied the decomposition kinetics of two carbonaceous materials: petroleum coke and synthetic graphite, added to a casting powder. Thermogravimetric (TG) data, obtained at different heating rates ($\beta = 5$, 7 10, 14 °C min^{-1}), were analyzed by non-isothermal kinetic methods to estimate both the activation energy of decomposition and the order of the reaction. A good correspondence of the activation energy of decomposition applying four non-isothermal methods was attained. For these models, the average activation energy corresponding to casting powder with 15 mass% of coke was lower than one with 15 mass% of graphite. Besides, a first order of reaction ($n = 1$) was assumed for the decomposition kinetic of both types of carbonaceous materials. A lower activation energy corresponding to the powder with coke was translated into higher reactivity of this powder compared to the sample with graphite. This fact would be taken into account during the mold powder design because higher reactivity is associated with higher melting rate.

In the present paper, a master decomposition curve (MDC) was constructed from the activation energy values. From the MDC, the time (t) needed to produce a specific degree of decomposition (α) at certain temperature (T) was calculated. The results predicted by this curve were experimentally verified. Thus, the present work is divided in two parts. The first part focuses on constructing the MDC of both carbonaceous materials, to estimate the degree of decomposition (or carbon removal) under different thermal conditions. Then, in the second part, the master curves were validated considering the mass loss of samples subjected to different heating schemes.

Theory

The theory of the decomposition master curve is a concept that can be used as a measure of the reaction of a set of particles. Based on this theory, it can be obtained a unique empirical curve predicting the behavior of the system under study, regardless heating rate [8, 9]. The MDC derives from the so-called master sintering curves (MSC) developed by Su and Johnson [10]. The MSC method has been applied to densification/sintering studies of several materials [11–14]. This concept was also used to develop master decomposition curves for thermal debinding of binders or polymer pyrolysis [15–17].

In [7], the thermal decomposition of both studied materials was assumed as the product of two functions: $k(T)$ depending on the absolute temperature T, and $f(\alpha)$ depending on the degree of decomposition α:

$$\frac{\mathrm{d}\alpha}{\mathrm{d}t} = k(T) \cdot f(\alpha) \tag{1}$$

According to the selected model, the conversion function $f(\alpha)$ can take several forms [18, 19]. On the other hand, the function $k(T)$ follows the Arrhenius equation:

$$k(T) = A \cdot \exp\left(-\frac{E}{R \cdot T}\right) \tag{2}$$

where A is the pre-exponential factor, E is the activation energy, and R is the gas constant. Thus, the reaction rate ($\mathrm{d}\alpha/\mathrm{d}t$) takes the form of Eq. 3:

$$\frac{\mathrm{d}\alpha}{\mathrm{d}t} = A \cdot \exp\left(-\frac{E}{R \cdot T}\right) \cdot f(\alpha) \tag{3}$$

Integrating this expression up to the decomposition value α:

$$\int_0^{\alpha} \frac{\mathrm{d}\alpha}{f(\alpha)} = A \cdot \int_0^{t} \exp\left(-\frac{E}{RT}\right) \cdot \mathrm{d}t = A \cdot \Theta_{\mathrm{D}} \tag{4}$$

where Θ_{D} is the work of decomposition and represents the energy to produce a certain degree of reaction α at temperature T during time t, and it is defined as:

$$\Theta_{\mathrm{D}}(E, T, t) = \int_0^{t} \exp\left(-\frac{E}{RT}\right) \cdot \mathrm{d}t \tag{5}$$

Considering the data obtained from the constant heating rate experiments $\beta = \mathrm{d}T/\mathrm{d}t$, Eq. 3 can be expressed as:

$$\frac{\mathrm{d}\alpha}{\mathrm{d}T} = \frac{A}{\beta} \cdot \exp\left(-\frac{E}{R \cdot T}\right) \cdot f(\alpha) \tag{6}$$

While Eq. 4 is transformed to:

$$\int_0^{\alpha} \frac{\mathrm{d}\alpha}{f(\alpha)} = A \cdot \int_{T_0}^{T} \frac{1}{\beta} \cdot \exp\left(-\frac{E}{RT}\right) \cdot \mathrm{d}T = A \cdot \Theta_{\mathrm{D}} \tag{7}$$

And

$$\Theta_D(E,T,\beta) = \int_{T_0}^{T} \frac{1}{\beta} \cdot \exp\left(-\frac{E}{RT}\right) \cdot dT \quad (8)$$

In this case, θ_D represents the energy to produce a mass loss fraction α when the material is heated at a constant rate β between the interval of temperature T_0 and T. The temperature T_0 represents the initial temperature of the decomposition process.

The integrand Q:

$$Q = \frac{1}{\beta} \cdot \exp\left(-\frac{E}{RT}\right) \quad (9)$$

is computed numerically.

Experimental

One commercial mold flux containing as major components: SiO_2 (31.0 mass%), CaO (27.0 mass%), Na_2O (11.0 mass%), Al_2O_3 (4.4 mass%), and F (9.0 mass%) was used as base material in this study. Commercial mold flux has a binary basicity (ratio CaO/SiO_2) of 0.87. This powder is used, in plant, for the casting of steels with medium carbon content. This casting powder was heated at 800 °C during 2 h for decarburization.

Two samples were prepared with the decarburizated mold flux, one adding 15 mass% of petroleum coke (sample C) and the other adding 15 mass% of synthetic graphite (sample G). Details of the process to obtain the compacts and thermogravimetric measurements were presented in [7]. Mass losses of both samples were determined at different heating rates (β = 5, 7, 10, and 14 °C min^{-1}) under a normal atmosphere. From these data, the degree of conversion (α) was calculated:

$$\alpha = \frac{W_S - w(t,T)}{W_S - W_F} \quad (10)$$

where W_S is the initial mass, W_F is the final mass, and $w(t, T)$ is the instantaneous mass.

Results and discussion

Construction of the MDCs

To construct the master decomposition curve, the values of both the activation energy (E) and the degree of decomposition (α), obtained from the thermogravimetric tests informed in [7], were used for each heating rate (β). Then, the work of decomposition (Θ_D) was calculated and the MDC was constructed from a sigmoidal fit.

In order to calculate the master curve, the following values of the activation energy were used: 46 ± 3 kJ mol^{-1} for the powder with coke and 63 ± 3 kJ mol^{-1} for the powder with graphite. These values of the activation energy of decomposition, corresponding to mean values of E, were calculated by four different isoconversional methods [7].

The decomposition work is obtained by plotting the integrand (Q) versus the absolute temperature T—see Eq. 8—between the initial (T_0) and the final temperature (T_F) of the reaction. Figure 1 shows an example of these graphs for the sample containing 15 wt% coke, heated at β = 10 °C min^{-1}, with different activation energies: 43, 46, and 49 kJ mol^{-1}. In this case, T_0 = 574 K and T_F = 1084 K were considered. The area under these curves is Θ_D (E, T, β).

In Fig. 2a, α values are plotted as a function of the logarithm of the decomposition work for the four different heating rates. Then, these four curves are averaged to obtain an average curve. Finally, this average curve is adjusted by means of a curve of sigmoidal type (Fig. 2b). As an example, Fig. 2 shows the master curve corresponding to sample C with an activation energy E = 46 kJ mol^{-1}.

The sigmoidal function used to fit the average curve was the following:

$$y = \frac{a}{1 + b \cdot \exp(-k \cdot x)} \quad (11)$$

where a, b, and k are parameters determined for each sample and for each activation energy. Table 1 lists these parameters obtained from sample G (E = 60, 63, and 66 kJ mol^{-1}) and sample C (E = 43, 46 and 49 kJ mol^{-1}).

Using this methodology, decomposition master curves are obtained for powders with coke and graphite, taking the different values of the activation energy: 43–49 kJ mol^{-1}

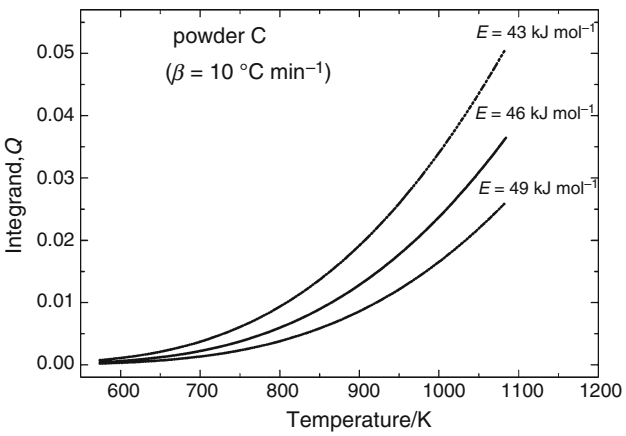

Fig. 1 Plots of integrand Q versus T for sample C at a heating rate of 10 °C min^{-1}

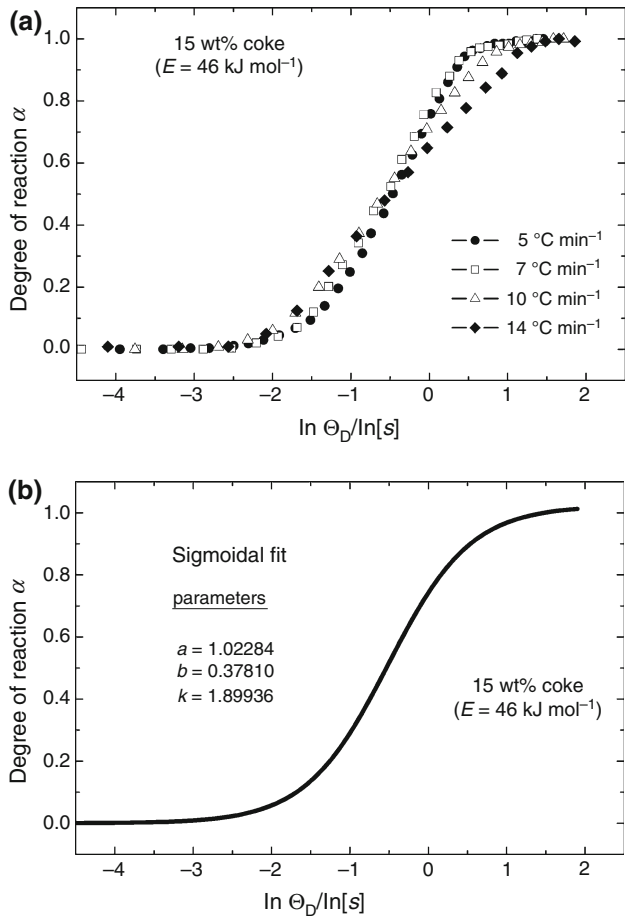

Fig. 2 **a** Plots of α versus ln Θ_D for sample C with $E = 46$ kJ mol^{-1}, and **b** fit sigmoidal of the average curve

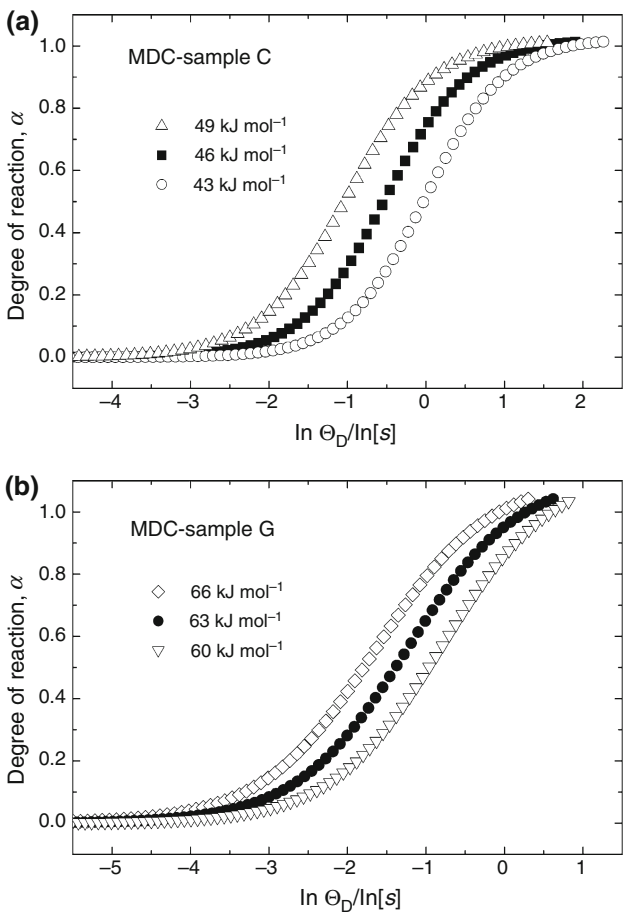

Fig. 3 Master decomposition curves of **a** sample C and **b** sample G

Table 1 Parameters corresponding to sigmoidal function (Eq. 11)

Sample G				Sample C			
E/kJ mol^{-1}	a	b	k	E/kJ mol^{-1}	a	b	k
60	1.13801	0.32547	1.42374	43	1.02554	0.98911	1.97420
63	1.11499	0.17039	1.42508	46	1.02284	0.37810	1.89936
66	1.10945	0.10015	1.39406	49	1.02040	0.15565	1.82849

for sample C (Fig. 3a) and between 60 and 66 kJ mol^{-1} for sample G (Fig. 3b).

Experimental validation of MDCs

Once the MDCs were obtained, experimental validation of these curves was performed. In this case, a value of α is selected (α-expected) and from the intersection with the master curve (Fig. 3), the value of the decomposition work is obtained. For this, Eq. 11 was used where $y = \alpha$ and $x = \ln \Theta_D$. Once the value of Θ_D is established for certain value of E, Eq. 5 is simplified to Eq. 12 when temperature T is constant:

$$\Theta_D(E, T, t) = \Delta t \cdot \exp\left(-\frac{E}{RT}\right) \quad (12)$$

From Eq. 12, it was possible to predict the time (Δt) needed to produce a given degree of decomposition (α) at different temperatures (T). In the present work, thermal treatments at $T = 500$, 600, 700 and 800 °C were selected. After each heat treatment, the mass loss of each sample was verified and experimental α values were obtained. Tables 2 and 3 show the expected and experimental values of α from samples G and C, respectively. These data were obtained at the indicated temperatures (column Temp, in °C) and times (column ΔT, in min:seg). Experimental data

Table 2 Experimental and expected values of α obtained under different heat treatments of powder G

Temp./°C	Δ*t* (min:seg)	α expected	α experimental
500	14:10	0.08	0.07
	25:15	0.16	0.10
600	14:10	0.30	0.31
	25:15	0.51	0.54
700	02:47	0.14	0.18
	04:16	0.23	0.23
	06:30	0.35	0.39
	10:01	0.48	0.43
	17:24	0.70	0.63
800	00:50	0.08	0.11
	04:32	0.44	0.32
	06:05	0.55	0.49
	16:39	0.91	0.74
	27:04	1.00	0.85

Table 3 Experimental and expected values of α obtained under different heat treatments of powder C

Temp./°C	Δ*t* (min:seg)	α expected	α experimental
500	07:34	0.30	0.35
	12:51	0.53	0.54
	25:15	0.80	0.82
600	00:23	0.01	0.02
	02:59	0.23	0.26
	03:44	0.32	0.30
	05:09	0.42	0.39
	11:16	0.78	0.62
700	01:29	0.22	0.19
	19:38	1.00	0.86
800	01:41	0.41	0.31
	01:53	0.47	0.34

listed in Tables 2 and 3 are plotted in Figs. 4 and 5, respectively.

As shown in Fig. 4 for powder G, experimental values of α are within the limits established by the master curves, except for a few samples for which $\alpha > 0.7$. Similar considerations are observed for samples with coke (Fig. 5).

This difference can also be seen in the curves of Fig. 2a, where it is observed that the greatest differences between the curves obtained at different heating rates are recorded for decomposition degree values (α) higher than 0.7. In [7], it is emphasized that the activation energy associated with

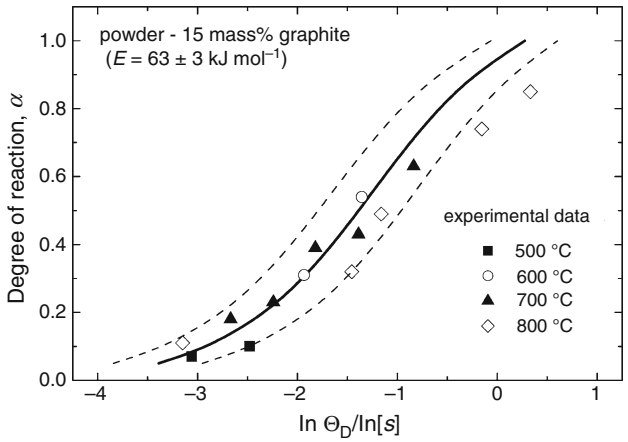

Fig. 4 Master curve and experimental data (points) obtained in sample G

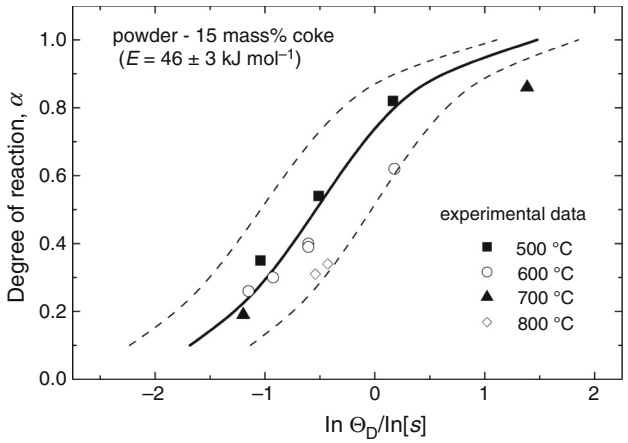

Fig. 5 Master curve and experimental data (points) obtained in sample C

the removal of carbon (as CO or CO_2 gas) tends toward lower values as the value of α increases. This departure from the mean value of *E*, for values of α greater than 0.7, is more pronounced in sample C. This behavior was associated with the fact that when the degree of reaction (α) exceeds 70%, the diffusion of the reaction products is carried out with less difficulty through a more open porous structure. Although the type of gas eliminated during the decomposition of carbonaceous materials has not been determined in the present work, it is assumed that reaction $C + O_2$ has the following products: CO_2, CO, H_2O and ash [20].

A greater presence of impurities or residual material (ash) in the coke could explain the greater difference in the values of the activation energy when the degree of decomposition progresses in sample C. That is, the decomposition kinetics (CO or CO_2 removal) in both materials may be acting with activation energies lower than

those used in the calculus of the present work when decomposition degree is > 0.7.

Final considerations

Although, in the present study, the chemical composition of both carbonaceous materials added to the casting powders has not been determined, it must be taken into account the higher content of ash presents in coke. Analysis of combustion of brick-shaped carbonaceous materials (carbon deposits, coke, and electrographite) under dynamic conditions [20] showed that the main difference between coke and deposits, and electrographite is ash content, which has catalytic influence on combustion rate (alkali compounds). Similarly, Li et al. [21] stated that addition of oxides has catalytic effect on oxidation reaction of graphite decreasing both the characteristic temperatures of the process and the activation energy.

In this research, the evolution of graphite flake morphology during the different stages of its decomposition was not followed, but the oxidation kinetics analyses of a natural graphite performed by Badenhorst et al. [22] are highlighted. They studied the application of both isothermal (between 600 and 700 °C in oxygen) and non-isothermal (heating rates of 1, 3 and 10 °C min^{-1} up to 1000 °C in air) analyses to the oxidation kinetics of this powdered graphite. The authors observed a larger error in the calculated values for the activation energy at low conversions ($\alpha < 0.1$) and a much larger spread in the values obtained for higher conversions ($\alpha > 0.65$) and attributed this behavior to the uncertainty of the data in these regions compared to central conversions ($0.1 < \alpha < 0.65$). They used an approach to model the gas–solid reaction of graphite and oxygen, and unexpected behavior was attributed to catalytic surface roughening as a result of the presence of trace metallic impurities. Subsequently, Badenhorst and Focke [23] studied changes in the morphologies of the flakes due to the oxidation reaction under isothermal conditions (650 °C in pure oxygen). They observed that the presence of catalytic impurities in two highly crystalline graphites developed macroscopic surface roughness during the initial stage of oxidation. Simulations based on simple geometric models supported the hypothesis that the conversion function is solely governed by the development of complex active surface area geometries.

Thus, the knowledge of the chemical composition of both carbonaceous materials and the products of their reaction with oxygen, together with the monitoring of the graphite flakes morphology, should be considered to elucidate the mechanisms responsible for the kinetics of decomposition of these carbonaceous materials.

Conclusions

To conclude, the following points developed in this article are worth highlighting:

1. A master decomposition curve was constructed from the carbon elimination kinetics associated with two carbonaceous materials: petroleum coke and synthetic graphite, added to a commercial casting powder.
2. Both master curves were validated by values of the degree of decomposition obtained from tests performed at different times and temperatures. Experimental data show a good correlation with those predicted theoretically by both master curves.
3. The use of this method based on MDC represents a useful tool to study the carbon elimination from this type of powders.

Acknowledgements The authors wish to thank Universidad Tecnológica Nacional (Argentina) for the financial support of this work.

References

1. Mills KC, Fox AB, Li Z, Thackray RP. Performance and properties of mould fluxes. Ironmak Steelmak. 2005;32:26–34.
2. Branion RV. Mold fluxes for continuous casting. Iron Steelmak. 1986;13:41–50.
3. Brandaleze E, Di Gresia G, Santini L, Martín A, Benavidez E. Mould fluxes in the steel continuous casting process. In: Srinivasan M, editor. Science and technology of casting processes. Rijeka: InTech; 2012. p. 205–33.
4. Kawamoto M, Nakajima K, Kanazawa T, Nakai K. Design principles of mold powder for high speed continuous casting. ISIJ Int. 1994;34:593–8.
5. Brandaleze E, Santini L, Gorosurreta C, Benavidez E, Martin A. Influence of carbonaceous particles on the melting behaviour of mold fluxes at high temperature. Proceedings 16° steelmaking conference IAS. San Nicolás, Argentina 2007; pp. 363–71.
6. Wei E, Yang Y, Feng C, Sommerville ID, McLean A. Effect of carbon properties on melting behavior of mold fluxes for continuous casting of steels. J Iron Steel Res. 2006;13:22–6.
7. Benavidez E, Santini L, Brandaleze E. Decomposition kinetic of carbonaceous materials used in a mold flux design. J Therm Anal Calorim. 2011;103:485–93.
8. Park SJ, German RM. Master curves based on time integration of thermal work in particulate materials. Int J Mater Struct Integr. 2007;1:128–46.
9. Diantonio CB, Ewsuk KG, Bencoe D. Extension of master sintering curve theory to organic decomposition. J Am Ceram Soc. 2005;88:2722–8.
10. Su H, Johnson DL. Master sintering curve: a practical approach to sintering. J Am Ceram Soc. 1996;79:3211–7.
11. Ewsuk KG, Ellerby DT, DiAntonio CB. Analysis of nanocrystalline and microcrystalline ZnO sintering using master sintering curves. J Am Ceram Soc. 2006;89:2003–9.
12. Caruso R, Mamana N, Benavidez E. Densification kinetics of ZrO_2-based ceramics using a master sintering curve. J Alloys Compd. 2010;495:570–3.

13. Bothara M, Atre SV, Park SJ, German RM, Sudarshan TS. Sintering behavior of nanocrystalline silicon carbide using a plasma pressure compaction system: master sintering curve analysis. Metall Mater Trans. 2010;41:3252–61.
14. Enneti RK, Bothara MB, Park SJ, Atre SV. Development of master sintering curve for field-assisted sintering of HfB2-20SiC. Ceram Int. 2012;38:4369–72.
15. Atre SV, Enneti RK, Park SJ, German RM. Master decomposition curve analysis of ethylene vinyl acetate pyrolisis: influence of metal powders. Powder Metall. 2008;51:368–75.
16. Aggarwal G, Park SJ, Smid I, German RM. Master decomposition curve for binders used in powder injection molding. Metall Mater Trans A. 2007;38:606–14.
17. Enneti RK, Shivashankar TS, Park SJ, German RM, Atre SV. Master debinding curves for solvent extraction of binders in powder injection molding. Powder Technol. 2012;228:14–7.
18. Chrissafis K. Kinetics of thermal degradation of polymers. J Therm Anal Calorim. 2009;95:273–83.
19. Sánchez-Jiménez PE, Criado JM, Pérez-Maqueda LA. Kissinger kinetic analysis of data obtained under different heating schedules. J Therm Anal Calorim. 2008;94:427–32.
20. Mianowski A, Bigda R, Zymla V. Study on kinetics of combustion of brick-shaped carbonaceous materials. J Therm Anal Calorim. 2006;84:563–74.
21. Li L, Tan Z-C, Meng S-H, Wang S-D, Wu D-Y. Kinetic study of the accelerating effect of coal-burning additives on the combustion of graphite. J Therm Anal Calorim. 2000;62:681–5.
22. Badenhorst H, Rand B, Focke WW. Modelling of natural graphite oxidation using thermal analysis techniques. J Therm Anal Calorim. 2010;99:211–28.
23. Badenhorst H, Focke WW. Geometric effects control isothermal oxidation of graphite flakes. J Therm Anal Calorim. 2012;108:1141–50.